HHS Public Access

Author manuscript

Mucosal Immunol. Author manuscript; available in PMC 2017 July 19.

Published in final edited form as:

Mucosal Immunol. 2017 September ; 10(5): 1133–1144. doi:10.1038/mi.2016.133.

Tryptophan Metabolite Activation of the Aryl Hydrocarbon Receptor Regulates IL10 Receptor Expression on Intestinal Epithelia

Jordi M. Lanis[1,2], **Erica E. Alexeev**[1,2], **Valerie F. Curtis**[1,2], **David A. Kitzenberg**[1,2], **Daniel J. Kao**[1,2], **Kayla D. Battista**[1,2], **Mark E. Gerich**[1,2], **Louise E. Glover**[1,2], **Douglas J. Kominsky**[1,3,#], and **Sean P. Colgan**[1,2,#]

[1]Mucosal Inflammation Program

[2]Department of Medicine, University of Colorado Anschutz Medical Campus, Aurora, CO

[3]Department of Microbiology and Immunology, Montana State University, Bozeman, MT

Abstract

IL10 is a potent anti-inflammatory cytokine that inhibits the production of pro-inflammatory mediators. Signaling by IL10 occurs through the IL10 receptor (IL10R), which is expressed in numerous cell types, including intestinal epithelial cells (IEC), where it is associated with development and maintenance of barrier function. Guided by an unbiased metabolomics screen, we identified tryptophan (Trp) metabolism as a major modifying pathway in IFN-γ-dominant murine colitis. In parallel, we demonstrated that IFN-γ induction of IDO1, an enzyme that catalyzes the conversion of Trp to kynurenine (Kyn), induces IL10R1 expression. Based on these findings, we hypothesized that IL10R1 expression on IEC is regulated by Trp metabolites. Analysis of the promoter region of IL10R1 revealed a functional aryl hydrocarbon response element (AHRE), which is induced by Kyn in luciferase-based IL10R1 promoter assays. Additionally, this analysis confirmed that IL10R1 protein levels were increased in response to Kyn in IEC *in vitro*. Studies utilizing *in vitro* wounding assays revealed that Kyn accelerates IL10-dependent wound closure. Finally, reduction of murine DSS colitis through Kyn administration correlates with colonic IL10R1 expression. Together, these results provide evidence on the importance of IL10 signaling in intestinal epithelia and implicate AHR in the regulation of IL10R1 expression in the colon.

*Correspondence to: Sean Colgan, Mucosal Inflammation Program, University of Colorado, Anschutz Medical Campus, 12700 East 19th Ave. MS B-146, Aurora, CO 80045, USA. Office phone: 303-724-7235 Fax: 303-724-7243 sean.colgan@ucdenver.edu or Douglas Kominsky, Department of Microbiology and Immunology, Montana State University, 109 Lewis Hall, Bozeman, MT 59717, USA. Office phone: 406-994-5667 Fax: 406-994-4926 douglas.kominsky@montana.edu.

#Co-senior authors

Author Contributions

J. Lanis designed and performed experiments, and wrote manuscript. E. Alexeev, V. Curtis, D. Kitzenberg, D. Kao, K. Battista, and M. Gerich performed experiments and edited the manuscript. L. Glover performed experiments. D. Kominsky and S. Colgan designed experiments, edited the manuscript, and oversaw the project.

Conflict of interest statement: The authors declare no financial interests in any of the work submitted here.

Keywords

mucosa; inflammation; metabolomics; wound healing; colitis

Introduction

A complex interdependency exists within the human intestine, where trillions of microbes interact with the host mucosa. While most of the microbiota benefit host health, pathogens and dysbiosis can lead to disease [1–5]. It is for this reason that a selective barrier is essential to intestinal homeostasis. Epithelial barrier is maintained through multiple levels of cell-cell interaction that functionally seals the epithelial monolayer. Defects in barrier function have been linked to many human diseases, most notably inflammatory bowel disease (IBD) [6].

The importance of IL10 signaling is well established in models of IBD. Indeed, mice lacking IL10 or the IL10 receptor are predisposed to spontaneous colitis [7–11]. Functional IL10 signaling in the epithelium promotes cell proliferation and barrier formation [12, 13], and results in homeostasis and maintenance of the epithelia (13). It was recently demonstrated that activation of the epithelial IFN-γ receptor, which is well established to induce barrier dysfunction [14, 15], also induces the expression of the IL10 receptor (IL10R1) in both cultured IEC and mice [13]. These results provide a compelling example of how balanced inflammatory processes also elicit inflammatory resolution.

One of the major signaling cascades induced by activation of IFN-γ receptors is induction of tryptophan (Trp) metabolism through the induction of indoleamine 2,3-dioxygenase (IDO1) [16, 17]. IDO1 is an enzyme responsible for conversion of Trp to kynurenine (Kyn) [18] and has been shown to suppress T cell proliferation through the localized catabolism of Trp [19]. Expression of IDO1 in intestinal epithelial cells strongly correlates with anti-inflammatory properties of dendritic cells [20–24], and reduces severity of colitis in mice [23]. Epithelial IDO1 has also been shown to activate β-catenin signaling and promote colonic tumorigenesis in inflammation-associated cancer [25].

Kyn is a Trp metabolite that functions as an endogenous ligand of the aryl hydrocarbon receptor (AHR) transcription factor [26, 27]. This transcription factor has been historically studied in the context of the synthetic dioxin based compound TCDD, and is known to control genes such as Cyp1A1 that are important for protecting cells from intoxication by various planar aromatic hydrocarbons [28, 29]. More recently, numerous endogenous ligands for AHR have been identified [30]. For example, Kyn competes with TCDD for binding cytosolic AHR and endogenously regulate systemic inflammation and tolerance [27]. Additionally, AHR has been implicated in various immune functions, including Th17 development and the expression of IL-17 and IL-22 [31–35]. Together, these data lead us to hypothesize that IFN-γ induces the expression of IL10R1 through an increase in tissue Trp metabolism and activation of AHR.

Results

Altered tissue metabolism in mice with DSS colitis

There is significant current interest in defining metabolomic changes associated with disease progression and inflammatory resolution [36]. Here, we performed a comprehensive, unbiased screen of metabolites of serum and colonic tissue from active DSS colitis. Mice were exposed to DSS via drinking water and serum and colonic epithelium were collected on day 7. Shown in Figure 1 is a summary of these results. This dataset comprised the analysis of 502 biochemicals of known identity. Principal component analysis revealed that metabolism was significantly altered both locally and systemically in mice administered DSS (Fig. 1A). In total, 42 metabolites were found to be significantly increased in the colon, while 120 metabolites were present in higher amounts in serum after DSS exposure. Most notable were changes in several metabolites along the Trp metabolism pathway in both serum and colons of colitic mice (Fig. 1B). Tryptophan is metabolized along at least 3 separate pathways involving various enzymatic signaling cascades and mechanisms (Fig. 1C). Catabolites of Trp were changed fundamentally in DSS colitis. In the colon, 5-hydroxyindoleacetate was significantly lower ($p<0.05$) while serotonin and C-glycosyltryptophan were increased ($p<0.05$, Fig. 1B). The most notable change was increased Kyn levels across both colon (4.4± 0.39-fold increase, $p<0.01$, Sup. Fig. 1) and serum samples (2.1±0.55 increase, $p<0.01$, Fig. 1B) from DSS colitic mice.

Elevated Kyn levels are associated with an upregulation of IDO1

In an attempt to better understand the temporal regulation of Kyn, independent analyses of Kyn levels in mice during various stages of DSS colitis were performed using EC-HPLC. Over the course of 7 days post DSS, Kyn levels increased in both the colon and serum compared to untreated mice (Fig. 2A, 2C). Kyn levels in the colon and serum gradually increased to over 7-fold the levels found at baseline with increasing time of exposure to DSS, supporting our LC-MS profiling screen (Fig. 2B, 2D). Interestingly, by day 10, Kyn levels in the colon and serum trend toward normal, suggesting that Kyn may serve as a sensitive biomarker of inflammation and resolution (Fig. 2B, 2D).

Once Trp is internalized, intracellular enzymes become the rate-limiting step in the catabolism of Trp to Kyn and other downstream metabolites. Consistent with previous studies in other cell types [37], analysis of our previously published microarray using T84 IEC [38] (GEO accession number GSE33880: http://www.ncbi.nlm.nih.gov/geo/query/acc.cgi?acc=GSE33880) revealed that the Trp catabolizing enzyme indoleamine 2,3-dioxygenase (IDO1) is highly upregulated upon exposure to IFN- γ (Fig. S1A), a cytokine that we have previously shown to be temporally upregulated in DSS colitis [13]. By contrast, other Trp catabolizing enzymes (e.g. TPH1 and TDO2) remain unchanged with IFN- γ treatment (Fig. S1A). In line with the data from IEC exposed to IFN- γ, mice had an increase in colonic IDO1 protein expression over a course of 10d of DSS and recovery as measured by western blot densitometry (Fig. 2E). IDO1 expression and subsequent Kyn production take place in a number of cell types including immune cells; therefore, we investigated whether isolated colonic epithelial cells upregulated IDO1 during DSS. DSS exposure lead to a 2-fold induction of *ido1* transcript levels in whole colon tissue, approximately a 3-fold induction

from colonic mucosal scrapings, and over a 10-fold induction of *ido1* transcript was detected in colonic epithelial cells enriched by immunomagnetic separation (Fig. 2F).

The primary known function of IDO1 is the conversion of Trp to Kyn. Therefore, we examined whether IFN- γ exposure increased Kyn levels in cultured IECs. As shown in Figure S1B, this analysis revealed that T84 cell exposure to IFN- γ resulted in a significant increase in secreted Kyn that can be inhibited by the tryptophan analog 1-methyl-DL-tryptophan (1-MT). IFN- γ has been shown to control expression of IL10R1 on IECs, so we also analyzed the expression of IL10R1 by qPCR in the presence of IFN- γ and 1-MT. While IFN- γ results in over a 50-fold increase in *il10r1* transcript, the presence of 1-MT skews the expression levels back toward baseline (Fig. S1C). We also measured transcript levels of a known AHR target, Cyp1A1, in the presence of 1-MT. Interestingly, without IDO1 tryptophan catabolism, Cyp1A1 levels return to baseline (Fig. S1C).

To further demonstrate the association between intestinal inflammation and elevated Kyn levels, we determined the levels of Kyn, IL10R1, and IDO1 in TNF(ΔARE) mice[39]. These mice develop a Crohn's disease-like pathology, and also show an increase in systemic Kyn, in line with data from the DSS treated mice (Fig. S2A). In turn, TNF(ΔARE) mice also have an increase in both *ido1* and *il10r1* mRNA in the colonic epithelia (Fig. S2B). Together, these results implicate a significant shift in Trp metabolism toward Kyn mediated by IFN- γ, and provide a link between IFN- γ signaling and the AHR pathway.

Expression of IL10R1 on IEC is controlled by AHR ligands

Given the strong association between IL10R1 and IFN- γ [13] and the above-described link between IFNγ and IDO1, we investigated the existence of a relationship between Trp metabolism and IL10R1 regulation in IEC. Kynurenine, along with other Trp metabolites, functions as an endogenous ligand for the aryl hydrocarbon receptor (AHR), a transcription factor that responds to planar aromatic hydrocarbons [27, 40, 41]. As shown in Figure 3, exposure of T84 IEC to Kyn, the UV-induced Trp derivative FICZ, and the AHR ligand TCDD resulted in a significant increase in both *il10r1* and *cyp1a1* mRNA levels (all $p < 0.05$, Fig. 3A). Analysis of the sequence flanking the IL10R1 gene identified several putative AHR response elements (5′-T/GNGCGTGA/CG/CA-3′) within the promoter region [42]. This 1.4 kb fragment of the promoter region was cloned upstream of a luciferase reporter, transfected into Caco-2 IEC, exposed to Kyn, FICZ, and IFN- γ and luciferase activity was measured after 12h. As shown in Figure 3B, FICZ, Kyn, and IFN- γ all significantly increased promoter activity compared to vehicle control ($p < 0.001$), suggesting that Trp metabolites induce IL10R1 through a mechanism involving AHR.

To further determine the influence of AHR on IL10R1 expression, we used short hairpin RNA knockdown (shRNA) to individually deplete AHR and the AHR nuclear transporter (ARNT) in Caco-2 and T84 IEC, respectively (Fig. S3A and S3B). Caco-2 AHR knockdown cells exposed to Kyn or FICZ resulted in no significant induction of IL10R1 compared to cells transfected with a non-targeting control shRNA (Fig. 3D–E). Similarly, T84 ARNT knockdown cells revealed no detectable levels of IL10R1 at baseline and no induction with FICZ, Kyn, or TCDD (Fig. 3F–G).

Expression of IL10R1 on IEC occurs predominantly on the apical surface of the cell [13]. To determine whether AHR ligand-induced AHR activation results in IL10R1 surface expression in adherent cells, we performed cell surface ELISA on Caco-2 shRNA control, ARNT KD cell lines, and Caco-2 cells treated with the pharmacological AHR inhibitor CH223191 (AHRi). In line with our western blot results, the expression of IL10R1 increased 8.96±2.06-fold ($p<0.01$) with FICZ, 4.38±1.06-fold ($p<0.05$) with Kyn, and 6.26±1.36-fold ($p<0.01$) with TCDD in shRNA control cells (Fig. 3C). No increase in IL10R1 was detectable with FICZ, Kyn, or TCDD exposure of ARNT KD or AHRi treated cells (p=not significant, Fig. 3C), further confirming a role for AHR/ARNT in the regulation of IL10R1 by Trp metabolites.

Previous work has shown a protective role for FICZ in murine models of colitis [32, 43]. We sought to determine how administration of FICZ *in vivo* might influence IL10R1 on the colonic mucosa. Villin-Cre+ conditional ARNT KO mice along with Cre- littermates were gavaged with 50 μg/kg of FICZ, and mRNA levels of IL10R1 in the colonic epithelia were analyzed after 6 h and 12 h. The *il10r1* mRNA levels were 2-fold higher (Fig. S4A) and the IL10R1 protein levels trended higher (Fig. S4 B–C) in the FICZ-treated control mice at 6 h and 12 h, respectively. Meanwhile, the ARNT KO mice showed no increase in *il10r1* transcript or protein expression (Fig. S4). By 12 h of FICZ exposure, *il10r1* levels in the Cre- mice returned to control levels, with no detectable change in ARNT KO tissue (Fig. S4). These results provide a compelling *in vivo* correlate for regulation of IEC IL10R1 by ARNT.

Activation of AHR promotes epithelial wound healing

We next determined whether AHR-dependent IL10R1 was functional. Our previous work demonstrated that IL10 signaling is important in IEC tight junction formation and ultimately barrier function; therefore, we performed an *in vitro* scratch wound assay using T84 IEC and followed the gap closure over 72 hours in the presence of a timed combination of Kyn followed by recombinant human IL10. As depicted in Figure 4A–B, scratch wounds closed by 82.7±4.0% over a 48 h period. The addition of Kyn alone resulted in a similar response to control monolayers (87.9±4.1%, p = not significant compared to control) while the addition of IL10 alone increased scratch wound closure to 93.6±3.2% ($p<0.05$ compared to control). The combination of Kyn and IL10 lead to 73.0±4.2% restitution by 24 h ($p<0.001$ compared to IL10 alone) and complete wound closure within 48 hours, indicating that Kyn-dependent signaling via IL10 functionally promotes epithelial wound closure independent of enhanced proliferation (Fig S5A).

By stark contrast, shRNA IL10R1 knockdown T84 cells exhibited delayed monolayer restitution in response to a combination of Kyn and IL10 (Fig. 4A–C). After 72 h, the mock treated control cells closed by only 54.9±7.4%, and the restitution with Kyn alone was not significant at 47.5±3.7% (Fig 4B). The addition of IL10 alone did not promote epithelial wound closure (63.5±6.7%) and the combination of Kyn and IL10 was not significantly different than mock treated control cells (66.4±4.6%). Similarly, another AHR ligand, FICZ, also promotes wound healing in T84 IEC in the presence of IL10 (Fig. 5A–C). However, ARNT KD IEC were unable to recover from the scratch wound regardless of FICZ or IL10

administration (Fig. 5B–C), indicating that the AHR/ARNT pathways appear to be essential for wound closure. In order to understand how the AHR ligands Kyn and FICZ are promoting wound healing, we next investigated whether the AHR ligands influenced expression of genes responsible for IEC junction proteins. T84 cells treated with Kyn or FICZ alone had no increase in any of the junctional genes assayed, indicating the observed wound healing is dependent on an increase in IL10 signaling and related downstream pathways (Fig. S5B). In turn, the lack of IL10R1 or ARNT abrogates the protective influences of the AHR–IL10 axis in IEC.

Exogenous Kyn protects mice from DSS colitis

AHR ligands such as FICZ have been shown to be protective in murine models of colitis through multiple mechanisms of immune cell modulation [32, 43]. Our data has shown that the AHR ligand Kyn is increased during inflammation through an upregulation of IDO1 and that this leads to IL10 receptor expression on intestinal epithelia. This increase in IL10R1 is associated with enhanced wound healing *in vitro*; therefore, we next explored the influence of Kyn supplementation in a murine model of DSS colitis. Eight-week-old C57–B6 mice were exposed to 2.5% DSS in the drinking water for 6 days, then recovered with tap water for 2 additional days. As shown in Fig. 6A–B, mice receiving Kyn (10mg/kg i.p.) loss less weight over 8 days, and had a substantial decrease in disease activity index (DAI). Despite the 10mg/kg dose of Kyn, the colonic and systemic levels of Kyn were measured to be no higher than the heightened physiologic levels seen during inflammation in Fig. 2 (Fig. S5 C–D). In line with the *in vitro* wound healing, DSS mice receiving Kyn display a significant reduction in intestinal permeability as measured by FITC-dextran (Fig. 6C). This protection in Kyn treated mice is extended to colon length (Fig. 6D–E). Colons in mice receiving DSS alone average 4.3±0.1 cm while colon length in Kyn treated DSS mice averaged 4.8±0.1 cm ($p<0.05$) (Fig. 6D–E). Histological analysis of the colon tissue revealed severe inflammation and loss of crypt architecture in DSS mice that is ameliorated with the addition of Kyn (Fig. 6F–G). These results are associated with increased IL10R1 expression in isolated colonic epithelial cells from mice receiving Kyn ($p<0.05$)(Fig. S6D).

In contrast, villin-cre+ conditional AHR knockout mice do not respond to Kyn during DSS colitis. As shown in Fig. S6A and S6C, there is no difference in disease activity or weight loss between DSS exposed AHR KO mice with or without Kyn. When compared to WT mice treated with Kyn, the AHR KO mice with Kyn consistently demonstrated more disease symptoms over the course of DSS and recovery ($p<0.001$) despite no difference in weight loss (Fig. S6B, S6D). In line with the results in Fig. 6, exposure to Kyn during DSS extended the colon lengths of Cre-negative control mice, while colons from AHR KO mice with or without Kyn are equal in length after DSS (Fig. S6E). Interestingly, colonic epithelial cells isolated from the AHR KO mice after DSS showed no increase in IL10R1 expression after Kyn treatment (Fig. S6F). Together, these results provide a mechanism for the protective influence of AHR signaling during colitis, and indicate that increased Kyn promotes barrier function through epithelial IL10 signaling.

Discussion

Intestinal epithelial cells function to both facilitate nutrient and fluid transport and provide the primary barrier to luminal antigens. Selective permeability is mediated by specialized anatomical features, including vectorial membrane transport systems and dynamically regulated intercellular junctions. Recent evidence suggests that during ongoing inflammation, pro-inflammatory signals (e.g. IFN- γ) elicit downstream responses that promote inflammatory resolution (e.g. induction of functional IL10 receptor) [13, 38, 44, 45]. It is clear that intestinal IL10 signaling is important for homeostasis and the lack of functional IL10/IL10R results in spontaneous colitis in mice [7–9]. Expression of the IL10 receptor on intestinal epithelial cells is associated with increased transepithelial resistance and barrier function [13]. In the current work, we define a role for IFN- γ-induced Trp metabolism in inflammation and identify the aryl hydrocarbon receptor (AHR) as the transcription factor responsible for IL10R1 expression in intestinal epithelia.

Inflammatory metabolism has become an area of intense interest [38]. Herein, we utilized an unbiased ananlysis to define metabolic shifts in ongoing intestinal inflammation. Initial metabolomic studies from mice with DSS colitis revealed that a number of the metabolites along the Trp metabolism pathway were altered both locally (i.e. colon) and systemically (serum). The elevation of Kyn in serum and colonic tissue during colitis was of particular interest. While we have not directly analyzed Kyn binding to AHR, others have shown that Kyn is a demonstrated endogenous ligand for AHR [26, 27] and can directly compete with TCDD for binding to cytosolic AHR [27]. Our previous work defined a prominent induction of IFN- γ in DSS colitis [13], and a major IFN- γ target is IDO1, a widely expressed protein that controls the catabolism of Trp to Kyn [38]. Increases in Trp metabolism through IDO1 can deplete local Trp levels and inhibit diverse functions, such as T cell proliferation [19] and intestinal bacterial growth [46, 47]. Our observations indicate that IFN- γ-induced IDO1 in IEC functions to increase levels of intracellular Kyn. It is notable that other branches of Trp metabolism (e.g. generation of serotonin) were also increased during active colitis (see Figure 1) and implicate a common metabolic process to promote the depletion of local Trp levels. Such metabolic regulation provides an important example of the intricate balance between inflammation and tissue metabolism.

Further investigation into the role of Trp metabolism in IEC revealed that various Trp metabolites induce IEC IL10R1. Both FICZ, a potent agonist of AHR, and Kyn induced IL10R1 expression both *in vitro* and *in vivo*, and activated an IL10R1 luciferase promoter construct. Extensions of these studies using loss of function strategies revealed that knockdown of either AHR or the AHR binding partner ARNT significantly attenuated FICZ-mediated induction of IL10R1. AHR was originally identified as the dioxin receptor, regulating genes important for response to various hydrocarbon toxicities [48, 49]. More recent studies have suggested that AHR may have a broader role in the regulation of a range of target genes, including a number of genes important in innate and adaptive immune responses as well as barrier properties on the skin and gut [50–52]. In fact, stimulation of AHR with FICZ has been shown to be protective in murine models of colitis [32, 43]. Our finding that IL10R1 is an AHR target in IEC, advances the mechanism(s) of anti-inflammation elicited by AHR activation.

The present findings also demonstrate a prominent role for IEC IL10R1 expression in wound healing. Our previous findings *in vitro* and *in vivo* identified a role for apically-localized IL10R1 in the regulation of epithelial barrier function [13]. Indeed, these studies revealed that shRNA-mediated knockdown of IL10R1 resulted in attenuated barrier formation and decreased baseline barrier function. Likewise, conditional deletion of IL10R1 in murine IEC resulted in increased intestinal permeability of healthy animals. Extension of these findings here to a scratch wound model revealed a prominent role for the IEC IL10R in control of wound healing. The combination of AHR ligand and IL10 significantly enhanced wound closure, thereby adding to our understanding of the protective role of IL10 during inflammatory processes.

Finally, administration of Kyn during DSS colitis demonstrated a protective role for Kyn increase during intestinal inflammation. Animals that received Kyn not only exhibited fewer physical signs of disease, but there was also significantly less damage to the crypt structure and intestinal barrier function. Kyn is an AHR ligand that can result in many physiological changes to the epithelia/immune cell axis. AHR responses by innate lymphoid cells and intraepithelial lymphocytes have also been shown to be protective during inflammation. Intraepithelial lymphocyte numbers are maintained through AHR stimulation from dietary ligands [53], and production of anti-inflammatory cytokines such as IL-22 by innate lymphoid cells in response to AHR ligands has been shown to be protective in colitis [32]. However, the direct response of the intestinal epithelia to these ligands is less understood. Studies in villin-cre AHR KO mice confirm that AHR expression within the intestinal epithelia is critical for protection from DSS via Kyn. The increase in IL10R1 in response to the AHR ligands FICZ and Kyn correlates with the decreased disease scores in Kyn treated WT mice, while the IL10R1 response to Kyn is abrogated in AHR KO mice. These results are also in line with the *in vitro* wound healing assays, demonstrating that increased epithelial IL10 receptor expression is vital for barrier protection and wound healing *in vivo*.

Taken together, these findings provide insight into the compelling protective role for AHR in the intestinal epithelium. Cumulatively, the data presented here clarify previous studies suggesting a protective role for Trp metabolism during ongoing inflammatory responses. Likewise, the data presented suggest that IFN- γ, via an IDO1-kyneurinine-AHR link, elicits adaptive mechanisms that promote a program of epithelial wound repair. The significance of these findings in patients is unclear at the present time. It is clear that IDO1 expression is increased in active IBD and that the serum Kyn:Trp ratio is increased in active Crohn's disease [54], suggesting that this metabolic pathway is active during disease. It could be postulated that inflammation-induced increases in IDO1 and the resulting Kyn act as a compensatory mechanism in patients with IBD.

Methods

Metabolomic Analysis

Distal colon tissue (1 cm) and serum were collected from control B6-129 mice and mice with DSS colitis. All tissues were flash frozen and global metabolomics was performed by Metabolon, Inc. (Durham, NC). Briefly, colon samples were removed from −80°C and weighed in tared cryovials and 80% MetOH was added at a ratio of 75μL solvent per mg of

sample, then incubated overnight at 4°C to extract biochemicals. Internal standards were included to control for extraction efficiency. Serum samples were prepared as previously described [55]. Following extraction in MetOH, both colon and serum samples were processed similarly and analyzed as described [55].

Animal Studies

For the metabolomics analyses, C57B6-129 crossed mice ages 8–12 weeks were given 3% (wt/vol) dextran sodium sulfate (DSS) (mol. weight 36,000–50,000; MP Biochemicals) in the drinking water for 5 days. After 5 days, normal tap water was returned for an additional 2 days before tissue collection. Control mice were maintained on tap water for 7 days. The DSS colitis model with Kyn supplementation was performed on C57B6 mice age 9 weeks as well as 9 week old AHR villin-cre+ and villin-cre− mice with 2.5% (wt/vol) DSS in the drinking water for 6 days. Aryl Hydrocarbon Receptor (AHR)–floxed (AHRfl/fl) mice containing loxP sites flanking exon 2 of the AHR gene[56] were crossbred to mice harboring the Cre-recombinase under control of the villin promoter (villin-Cre mice; Jackson Laboratories). Mice receiving Kyn were injected i.p. with 10 mg/kg of kynurenine sulfate salt (Sigma) in PBS at day 0 and every 48 h thereafter. Control mice received PBS injections only. After 6 days, normal tap water was returned for an additional 2 days before tissue collection. Body weight, occult blood in feces, and stool consistency were recorded daily to determine DAI as previously described[57]. Aryl Hydrocarbon Receptor Nuclear Transporter (ARNT)–floxed (ARNTfl/fl) mice containing loxP sites flanking exon 6 of the ARNT gene[58] (Jackson Laboratories, Bar Harbor, ME) were crossbred to mice harboring the Cre-recombinase under control of the villin promoter (villin-Cre mice; Jackson Laboratories). Genotyping of mice was carried out as described previously. Eight to 12 week old female mice were gavaged with 50 μg/kg FICZ emulsified in 40% (2-hydroxypropyl)-beta-cyclodextrin (HPβCD) (ArozTech) or HPβCD alone 6 h and 12 h prior to tissue collection. Cre-negative littermates were used as controls. Tissues from 24 week old TNF(deltaARE) mice were harvested to analyze Kyn, IDO1, and IL10R1 [39]. All animal work was approved by the Institutional Animal Care and Use Committee at the University of Colorado.

Tissue Collection, Processing, and FITC-dextran permeability

Colons with attached ceca were removed and measured. Approximately 1 cm of whole colon or epithelial scraping was removed and placed in Tris lysis buffer for protein analysis, RNAlater (Ambion) for qPCR, or flash frozen in liquid nitrogen for HPLC analysis. Isolated epithelial cells were processed using EasySep mouse epithelial enrichment kit (Stem Cell Technologies). Subsequently, RNA was isolated using RNeasy (Qiagen). Four hours prior to tissue collection, mice were gavaged with 100 mg of 4 kd FITC-dextran in PBS. Blood for serum analysis was collected via cheek bleeds into serum collection tubes (Sarstedt), centrifuged at 5000 x g, and 50 μL of serum diluted 1:2 in PBS and placed into wells of a black walled, clear bottom 96-well plate. Fluorescence was measured using a Promega fluorescent plate reader at ex. 490 em. 525, and compared to a standard curve.

Histological scoring

Histological examination was performed on three samples of the distal colon. Samples were fixed in 10% formalin before staining with hematoxylin and eosin. All histological

quantitation was performed in a blinded fashion, using a previously described scoring system [59]. The three independent parameters measured were severity of inflammation (0–3: none, slight, moderate, severe), extent of injury (0–3: none, mucosal, mucosal and submucosal, transmural), and crypt damage (0–4: none, basal 1/3 damaged, basal 2/3 damaged, only surface epithelium intake, entire crypt and epithelium lost). The score of each parameter was multiplied by a factor reflecting the percentage of tissue involvement (x1: 0–25%, x2: 26–50%, x3: 51–75%, x4: 76–100%) and all numbers were summed. Maximum possible score was 40.

Cell Lines and shRNA Knockdown

Human T84 and Caco-2 intestinal epithelial cells (IEC) were cultured in 1:1 DMEM-Ham's F12 with 2.5 mM L-glutamine and 10% FBS and DMEM with 20% FBS respectively. Cells were maintained at 37°C with 5% CO_2. Lentiviral particles encoding shRNA directed against ARNT, AHR, and IL10R1 (MISSION TRC shRNA, Sigma) were used to transduce Caco-2 and T84 cells using standard protocols. Stable integration was achieved by puromycin selection (6 μg/mL). Knockdown was confirmed by qPCR analysis, indicating 85% depletion of both ARNT and AHR levels, and 79% depletion of IL10R1. For mRNA and protein analysis, cells were grown to confluence on 5 cm^2 permeable supports to form polarized monolayers. Where indicated, cells were treated with the AHR inhibitor CH223191 (Sigma, 10 μM), the IDO1 inhibitor 1-methyl-DL-tryptophan (1-MT, Sigma), recombinant human IFN- γ (10 ng/mL, R&D), or the AHR agonists FICZ (6-Formylindolo(3,2-b)carbazole; 100 nM – 1 μM; Enzo), Kyn (Kynurenine, Sigma, 100 μM), or TCDD (2,3,7,8-tetrachlorodibenzo-p-dioxin, Sigma, 30 nM) in serum free media.

EC-HPLC Metabolite Analysis

Kyn and Trp derivatives were quantified using isocratic reversed-phase high-performance liquid chromatography with electrochemical coulometric array detection (EC-HPLC) (Coularray, Thermo Scientific, Waltham, MA). Both tissue and cell samples were extracted in 6% perchloric acid and protein precipitate and cell debris was removed by centrifugation at 12,000x g. Separation was achieved using an Acclaim Polar Advantage II C18 column, 5 μm 120Å, 4.6 x 150 mm, (Thermo) at a flow rate of 1 to 1.5 mL/min in a mobile phase consisting of 10% acetonitrile in 50 mM sodium phosphate buffer, pH 3, containing 0.42 mM octanesulphonic acid as an ion-pairing agent. The data were quantified using the Coularray software in comparison to standards.

Real-time PCR

Total RNA was extracted from cells using TRIzol (Invitrogen) and cDNA was prepared using the iSCRIPT cDNA synthesis kit (Bio-Rad). Real-time PCR to measure IL10R1 transcript was performed in 1× Power SYBR Green master mix (Applied Biosystems) using an ABI 7300 thermocycler. Fold change in expression of target mRNA relative to β-actin mRNA was calculated as previously outlined [60]. Primer sequences: human IL10R1 F-CCCTGTCCTATGACCTTACCG R-CACACTGCCAACTGTCAGAGT, human Cyp1A1 F-ACCCGCCACCCTTCGACAGTTC R-TGCCCAGGCGTTGCGTGAGAAG, human Cyp1B1 F-CTGGCACTGACGACGCCAAGAGACT R-TGGTCTGCTGGATGGACAGCGGGTT, mouse IL10R1 F- CCCATTCCTCGTCACGATC

R- TCAGACTGGTTTGGGATAGGTTT, mouse IDO1, F-TGGCGTATGTGTGGAACCG R-CTCGCAGTAGGGAACAGCAA, human β-catenin (β-CAT) F-AAAATGGCAGTGCGTTTAG R-TTTGAAGGCAGTCTGTCGTA, human Claudin 1 (CLDN1) F- CCAGTCAATGCCAGGTACGAAT R- TTGGTGTTGGGTAAGAGGTTGTT, human E-Cadherin (E-Cad) F- GCCCATTTCCTAAAAACCTG R-CTCTGTCACCTTCAGCCATC, human JAMA F- CCTGGGAATCTTGGTTTTTG R-GGAATGACGAGGTCTGTTTG, human occludin (OCC) F-GCTACGGAAGTGGCTATGG R- GCGGCAATGAAACAAAAG, human ZO-1 F-TGGTGTCCTACCTAATTCAACTCA R-CGCCAGCTACAAATATTCCAACA.

Western Blot and Cell Surface ELISA

Whole cell lysate was extracted in RIPA buffer on ice. Mouse colon samples were collected in Tris lysis buffer and sonicated until homogenous. Protein content was quantified using BCA protein assay reagent (Thermoscientific) and 25 μg of whole cell extract was boiled in Laemmli buffer in reducing conditions and subjected to SDS/PAGE. The SDS/PAGE was transferred onto PVDF and probed for human IL10R1 using a rabbit polyclonal IL10RA antibody (Thermo), mouse IL10R1 using a rabbit polyclonal IL10RA antibody (Millipore), mouse IDO1 antibody (Cell Signaling), human ARNT antibody (BD Labs), human AHR antibody (Cell Signaling), and β-actin (Abcam) according to manufacturer's recommendations. Densitometry analysis was performed using ImageJ software (http://imagej.nih.gov/ij, NIH). Confluent monolayers of Caco-2 cells containing a non-template control (shNTC) or shRNA specific for ARNT were treated with FICZ (1 μM) for 24 h, fixed with 4% PFA, blocked in 10% BSA in PBS, and stained using a rabbit polyclonal IL10RA antibody (Millipore) at 1:200 overnight at 4°C. The IL10RA antibody was detected using an HRP-linked secondary antibody, a TMB peroxidase substrate (KPL), and reactivity measured at a wavelength of 450nm.

Plasmids, Transfection, and Luciferase Assays

The 5′ flanking promoter sequence of the IL10R1 gene (from −994 to +23 bp) was amplified from human genomic DNA and subcloned into the pGL3–basic luciferase reporter vector (Promega) to generate pIL10R1-Luc. Caco-2 cells were seeded into 24-well dishes and transfected with the luciferase reporter plasmid pIL10R1-Luc or empty pGL3-basic-Luc (100 ng) using Lipofectamine-LTX (Invitrogen). To assay promoter activity, cells were exposed to 1 μM FICZ, 100 μM Kyn, or 10 ng/mL IFN- γ 24 h posttransfection and harvested at 48 h posttransfection and luciferase activity was measured in extracts using the Dual-Glo luciferase reporter kit and GloMax system (Promega). All firefly luciferase activity was normalized to a cotransfected pRL-SV40 Renilla luciferase reporter (Promega).

Cell proliferation Assay

T84 IEC were seeded into 96-well plates at a low density of 5,000 cells per well, allowed to settle, and immediately treated with 250 nM FICZ, 100 μM Kyn, 10 ng/mL IL10, vehicle, or a combination. Cell proliferation was measured in relation to dehydrogenase activity as measured by the CCK-8 assay (Dojindo), according to manufacturer's instructions.

Scratch Wound Assay

T84 shNTC, shIL10R1 kd, and shARNT kd cells were seeded into 6-well dishes and grown to confluence. One cm length wounds were scratched into the epithelia using a 10 μl pipette tip and the scratches were monitored daily at 10x using a Nikon. Cells were treated daily with fresh media, 250 nM FICZ, 100 μM Kyn, and/or 10 ng/mL IL10. Wound width was measured in 3 places within the same field over 72 h using Spot software (Spot Imaging).

Statistical Analysis

Data are expressed as the means ± S.E.M. Statistical analyses were performed using two-tailed unpaired Student's t-test in GraphPad Prism (La Jolla, CA) for direct comparisons, one-way ANOVA with Tukey's test for multiple comparisons, and two-way ANOVA with Sidak's multiple comparison and multiple t-test for grouped data. Statistical significance is reported as * $p<0.05$, ** $p<0.01$, *** $p<0.001$.

Supplementary Material

Refer to Web version on PubMed Central for supplementary material.

Acknowledgments

This work was supported by NIH grants DK099452, DK50189, DK095491, VA Merit BX002182 and by the Crohn's and Colitis Foundation of America.

References

1. Candela M, Perna F, Carnevali P, Vitali B, Ciati R, Gionchetti P, et al. Interaction of probiotic Lactobacillus and Bifidobacterium strains with human intestinal epithelial cells: adhesion properties, competition against enteropathogens and modulation of IL-8 production. International journal of food microbiology. 2008; 125(3):286–292. [PubMed: 18524406]
2. Lozupone CA, Stombaugh JI, Gordon JI, Jansson JK, Knight R. Diversity, stability and resilience of the human gut microbiota. Nature. 2012; 489(7415):220–230. [PubMed: 22972295]
3. Fukuda S, Toh H, Hase K, Oshima K, Nakanishi Y, Yoshimura K, et al. Bifidobacteria can protect from enteropathogenic infection through production of acetate. Nature. 2011; 469(7331):543–547. [PubMed: 21270894]
4. Olszak T, An D, Zeissig S, Vera MP, Richter J, Franke A, et al. Microbial exposure during early life has persistent effects on natural killer T cell function. Science (New York, NY). 2012; 336(6080): 489–493.
5. Sonnenburg JL, Xu J, Leip DD, Chen CH, Westover BP, Weatherford J, et al. Glycan foraging in vivo by an intestine-adapted bacterial symbiont. Science (New York, NY). 2005; 307(5717):1955–1959.
6. Xavier RJ, Podolsky DK. Unravelling the pathogenesis of inflammatory bowel disease. Nature. 2007; 448(7152):427–434. [PubMed: 17653185]
7. Chaudhry A, Samstein RM, Treuting P, Liang Y, Pils MC, Heinrich JM, et al. Interleukin-10 signaling in regulatory T cells is required for suppression of Th17 cell-mediated inflammation. Immunity. 2011; 34(4):566–578. [PubMed: 21511185]
8. Kuhn R, Lohler J, Rennick D, Rajewsky K, Muller W. Interleukin-10-deficient mice develop chronic enterocolitis. Cell. 1993; 75(2):263–274. [PubMed: 8402911]
9. Pils MC, Pisano F, Fasnacht N, Heinrich JM, Groebe L, Schippers A, et al. Monocytes/macrophages and/or neutrophils are the target of IL-10 in the LPS endotoxemia model. European journal of immunology. 2010; 40(2):443–448. [PubMed: 19941312]

10. Engelhardt KR, Grimbacher B. IL-10 in humans: lessons from the gut, IL-10/IL-10 receptor deficiencies, and IL-10 polymorphisms. Current topics in microbiology and immunology. 2014; 380:1–18. [PubMed: 25004811]
11. Glocker EO, Kotlarz D, Boztug K, Gertz EM, Schaffer AA, Noyan F, et al. Inflammatory bowel disease and mutations affecting the interleukin-10 receptor. The New England journal of medicine. 2009; 361(21):2033–2045. [PubMed: 19890111]
12. Loren V, Cabre E, Ojanguren I, Domenech E, Pedrosa E, Garcia-Jaraquemada A, et al. Interleukin-10 Enhances the Intestinal Epithelial Barrier in the Presence of Corticosteroids through p38 MAPK Activity in Caco-2 Monolayers: A Possible Mechanism for Steroid Responsiveness in Ulcerative Colitis. PloS one. 2015; 10(6):e0130921. [PubMed: 26090671]
13. Kominsky DJ, Campbell EL, Ehrentraut SF, Wilson KE, Kelly CJ, Glover LE, et al. IFN-gamma-mediated induction of an apical IL-10 receptor on polarized intestinal epithelia. Journal of immunology (Baltimore, Md : 1950). 2014; 192(3):1267–1276.
14. Mankertz J, Tavalali S, Schmitz H, Mankertz A, Riecken EO, Fromm M, et al. Expression from the human occludin promoter is affected by tumor necrosis factor alpha and interferon gamma. Journal of cell science. 2000; 113:2085–2090. [PubMed: 10806119]
15. Youakim A, Ahdieh M. Interferon-gamma decreases barrier function in T84 cells by reducing ZO-1 levels and disrupting apical actin. The American journal of physiology. 1999; 276(5 Pt 1):G1279–1288. [PubMed: 10330020]
16. Yoshida R, Imanishi J, Oku T, Kishida T, Hayaishi O. Induction of pulmonary indoleamine 2,3-dioxygenase by interferon. Proceedings of the National Academy of Sciences. 1981; 78(1):129–132.
17. Yasui H, Takai K, Yoshida R, Hayaishi O. Interferon enhances tryptophan metabolism by inducing pulmonary indoleamine 2,3-dioxygenase: its possible occurrence in cancer patients. Proceedings of the National Academy of Sciences. 1986; 83(17):6622–6626.
18. Higuchi K, Hayaishi O. Enzymic formation of D-kynurenine from D-tryptophan. Archives of biochemistry and biophysics. 1967; 120(2):397–403. [PubMed: 4291827]
19. Munn DH, Shafizadeh E, Attwood JT, Bondarev I, Pashine A, Mellor AL. Inhibition of T cell proliferation by macrophage tryptophan catabolism. The Journal of experimental medicine. 1999; 189(9):1363–1372. [PubMed: 10224276]
20. Matteoli G, Mazzini E, Iliev ID, Mileti E, Fallarino F, Puccetti P, et al. Gut CD103+ dendritic cells express indoleamine 2,3-dioxygenase which influences T regulatory/T effector cell balance and oral tolerance induction. Gut. 2010; 59(5):595–604. [PubMed: 20427394]
21. Nguyen NT, Kimura A, Nakahama T, Chinen I, Masuda K, Nohara K, et al. Aryl hydrocarbon receptor negatively regulates dendritic cell immunogenicity via a kynurenine-dependent mechanism. Proceedings of the National Academy of Sciences of the United States of America. 2010; 107(46):19961–19966. [PubMed: 21041655]
22. Pallotta MT, Orabona C, Volpi C, Vacca C, Belladonna ML, Bianchi R, et al. Indoleamine 2,3-dioxygenase is a signaling protein in long-term tolerance by dendritic cells. Nature immunology. 2011; 12(9):870–878. [PubMed: 21804557]
23. Ciorba MA, Bettonville EE, McDonald KG, Metz R, Prendergast GC, Newberry RD, et al. Induction of IDO-1 by immunostimulatory DNA limits severity of experimental colitis. Journal of immunology (Baltimore, Md : 1950). 2010; 184(7):3907–3916.
24. Muzaki AR, Tetlak P, Sheng J, Loh SC, Setiagani YA, Poidinger M, et al. Intestinal CD103CD11b dendritic cells restrain colitis via IFN-gamma-induced anti-inflammatory response in epithelial cells. Mucosal immunology. 2015
25. Thaker AI, Rao MS, Bishnupuri KS, Kerr TA, Foster L, Marinshaw JM, et al. IDO1 metabolites activate beta-catenin signaling to promote cancer cell proliferation and colon tumorigenesis in mice. Gastroenterology. 2013; 145(2):416–425. e411–414. [PubMed: 23669411]
26. Opitz CA, Litzenburger UM, Sahm F, Ott M, Tritschler I, Trump S, et al. An endogenous tumour-promoting ligand of the human aryl hydrocarbon receptor. Nature. 2011; 478(7368):197–203. [PubMed: 21976023]

27. Bessede A, Gargaro M, Pallotta MT, Matino D, Servillo G, Brunacci C, et al. Aryl hydrocarbon receptor control of a disease tolerance defence pathway. Nature. 2014; 511(7508):184–190. [PubMed: 24930766]
28. Fernandez-Salguero PM, Hilbert DM, Rudikoff S, Ward JM, Gonzalez FJ. Aryl-hydrocarbon receptor-deficient mice are resistant to 2,3,7,8-tetrachlorodibenzo-p-dioxin-induced toxicity. Toxicology and applied pharmacology. 1996; 140(1):173–179. [PubMed: 8806883]
29. Gielen JE, Goujon FM, Nebert DW. Genetic regulation of aryl hydrocarbon hydroxylase induction. II. Simple Mendelian expression in mouse tissues in vivo. The Journal of biological chemistry. 1972; 247(4):1125–1137. [PubMed: 4110756]
30. Nguyen LP, Bradfield CA. The Search for Endogenous Activators of the Aryl Hydrocarbon Receptor. Chemical research in toxicology. 2008; 21(1):102–116. [PubMed: 18076143]
31. Monteleone I, MacDonald TT, Pallone F, Monteleone G. The aryl hydrocarbon receptor in inflammatory bowel disease: linking the environment to disease pathogenesis. Current opinion in gastroenterology. 2012; 28(4):310–313. [PubMed: 22450895]
32. Monteleone I, Rizzo A, Sarra M, Sica G, Sileri P, Biancone L, et al. Aryl hydrocarbon receptor-induced signals up-regulate IL-22 production and inhibit inflammation in the gastrointestinal tract. Gastroenterology. 2011; 141(1):237–248. 248e231. [PubMed: 21600206]
33. Mascanfroni ID, Takenaka MC, Yeste A, Patel B, Wu Y, Kenison JE, et al. Metabolic control of type 1 regulatory T cell differentiation by AHR and HIF1-alpha. Nature medicine. 2015; 21(6): 638–646.
34. Heller JJ, Qiu J, Zhou L. Nuclear receptors take center stage in Th17 cell-mediated autoimmunity. The Journal of clinical investigation. 2011; 121(2):519–521. [PubMed: 21266768]
35. Kimura A, Naka T, Nohara K, Fujii-Kuriyama Y, Kishimoto T. Aryl hydrocarbon receptor regulates Stat1 activation and participates in the development of Th17 cells. Proceedings of the National Academy of Sciences of the United States of America. 2008; 105(28):9721–9726. [PubMed: 18607004]
36. Colgan SP, Campbell EL, Kominsky DJ. Hypoxia and Mucosal Inflammation. Ann Rev Pathol. 2016; 11:77–100. [PubMed: 27193451]
37. Taylor MW, Feng GS. Relationship between interferon-gamma, indoleamine 2,3-dioxygenase, and tryptophan catabolism. FASEB journal : official publication of the Federation of American Societies for Experimental Biology. 1991; 5(11):2516–2522. [PubMed: 1907934]
38. Kominsky DJ, Keely S, MacManus CF, Glover LE, Scully M, Collins CB, et al. An endogenously anti-inflammatory role for methylation in mucosal inflammation identified through metabolite profiling. Journal of immunology (Baltimore, Md : 1950). 2011; 186(11):6505–6514.
39. Kontoyiannis D, Pasparakis M, Pizarro TT, Cominelli F, Kollias G. Impaired on/off regulation of TNF biosynthesis in mice lacking TNF AU-rich elements: implications for joint and gut-associated immunopathologies. Immunity. 1999; 10(3):387–398. [PubMed: 10204494]
40. Poland A, Clover E, Kende AS, DeCamp M, Giandomenico CM. 3,4,3′,4′-Tetrachloro azoxybenzene and azobenzene: potent inducers of aryl hydrocarbon hydroxylase. Science (New York, NY). 1976; 194(4265):627–630.
41. Wincent E, Bengtsson J, Mohammadi Bardbori A, Alsberg T, Luecke S, Rannug U, et al. Inhibition of cytochrome P4501-dependent clearance of the endogenous agonist FICZ as a mechanism for activation of the aryl hydrocarbon receptor. Proceedings of the National Academy of Sciences of the United States of America. 2012; 109(12):4479–4484. [PubMed: 22392998]
42. Bacsi SG, Reisz-Porszasz S, Hankinson O. Orientation of the heterodimeric aryl hydrocarbon (dioxin) receptor complex on its asymmetric DNA recognition sequence. Molecular pharmacology. 1995; 47(3):432–438. [PubMed: 7700240]
43. Ji T, Xu C, Sun L, Yu M, Peng K, Qiu Y, et al. Aryl Hydrocarbon Receptor Activation Down-Regulates IL-7 and Reduces Inflammation in a Mouse Model of DSS-Induced Colitis. Digestive diseases and sciences. 2015; 60(7):1958–1966. [PubMed: 25799939]
44. Kelchtermans H, Billiau A, Matthys P. How interferon-gamma keeps autoimmune diseases in check. Trends in immunology. 2008; 29(10):479–486. [PubMed: 18775671]

45. Sheikh SZ, Matsuoka K, Kobayashi T, Li F, Rubinas T, Plevy SE. Cutting edge: IFN-gamma is a negative regulator of IL-23 in murine macrophages and experimental colitis. Journal of immunology (Baltimore, Md : 1950). 2010; 184(8):4069–4073.
46. Carlin JM, Ozaki Y, Byrne GI, Brown RR, Borden EC. Interferons and indoleamine 2,3-dioxygenase: role in antimicrobial and antitumor effects. Experientia. 1989; 45(6):535–541. [PubMed: 2472288]
47. MacKenzie CR, Langen R, Takikawa O, Daubener W. Inhibition of indoleamine 2,3-dioxygenase in human macrophages inhibits interferon-gamma-induced bacteriostasis but does not abrogate toxoplasmastasis. European journal of immunology. 1999; 29(10):3254–3261. [PubMed: 10540337]
48. Poland AP, Glover E, Robinson JR, Nebert DW. Genetic expression of aryl hydrocarbon hydroxylase activity. Induction of monooxygenase activities and cytochrome P1-450 formation by 2,3,7,8-tetrachlorodibenzo-p-dioxin in mice genetically “nonresponsive” to other aromatic hydrocarbons. The Journal of biological chemistry. 1974; 249(17):5599–5606. [PubMed: 4370044]
49. Xu C, Li CY, Kong AN. Induction of phase I, II and III drug metabolism/transport by xenobiotics. Archives of pharmacal research. 2005; 28(3):249–268. [PubMed: 15832810]
50. Fernandez-Salguero P, Pineau T, Hilbert DM, McPhail T, Lee SS, Kimura S, et al. Immune system impairment and hepatic fibrosis in mice lacking the dioxin-binding Ah receptor. Science (New York, NY). 1995; 268(5211):722–726.
51. Esser C, Rannug A, Stockinger B. The aryl hydrocarbon receptor in immunity. Trends in immunology. 2009; 30(9):447–454. [PubMed: 19699679]
52. Esser C, Rannug A. The aryl hydrocarbon receptor in barrier organ physiology, immunology, and toxicology. Pharmacological reviews. 2015; 67(2):259–279. [PubMed: 25657351]
53. Li Y, Innocentin S, Withers DR, Roberts NA, Gallagher AR, Grigorieva EF, et al. Exogenous stimuli maintain intraepithelial lymphocytes via aryl hydrocarbon receptor activation. Cell. 2011; 147(3):629–640. [PubMed: 21999944]
54. Gupta NK, Thaker AI, Kanuri N, Riehl TE, Rowley CW, Stenson WF, et al. Serum analysis of tryptophan catabolism pathway: correlation with Crohn’s disease activity. Inflammatory bowel diseases. 2012; 18(7):1214–1220. [PubMed: 21823214]
55. Albrecht E, Waldenberger M, Krumsiek J, Evans AM, Jeratsch U, Breier M, et al. Metabolite profiling reveals new insights into the regulation of serum urate in humans. Metabolomics : Official journal of the Metabolomic Society. 2014; 10(1):141–151. [PubMed: 24482632]
56. Walisser JA, Glover E, Pande K, Liss AL, Bradfield CA. Aryl hydrocarbon receptor-dependent liver development and hepatotoxicity are mediated by different cell types. Proc Natl Acad Sci U S A. 2005; 102(49):17858–17863. [PubMed: 16301529]
57. Frick JS, MacManus CF, Scully M, Glover LE, Eltzschig HK, Colgan SP. Contribution of adenosine A2B receptors to inflammatory parameters of experimental colitis. J Immunol. 2009; 182(8):4957–4964. [PubMed: 19342675]
58. Tomita S, Sinal CJ, Yim SH, Gonzalez FJ. Conditional disruption of the aryl hydrocarbon receptor nuclear translocator (Arnt) gene leads to loss of target gene induction by the aryl hydrocarbon receptor and hypoxia-inducible factor 1alpha. Mol Endocrinol. 2000; 14(10):1674–1681. [PubMed: 11043581]
59. Dieleman LA, Palmen MJ, Akol H, Bloemena E, Pena AS, Meuwissen SG, et al. Chronic experimental colitis induced by dextran sulphate sodium (DSS) is characterized by Th1 and Th2 cytokines. Clin Exp Immunol. 1998; 114(3):385–391. [PubMed: 9844047]
60. Pfaffl MW. A new mathematical model for relative quantification in real-time RT-PCR. Nucleic acids research. 2001; 29(9):e45. [PubMed: 11328886]

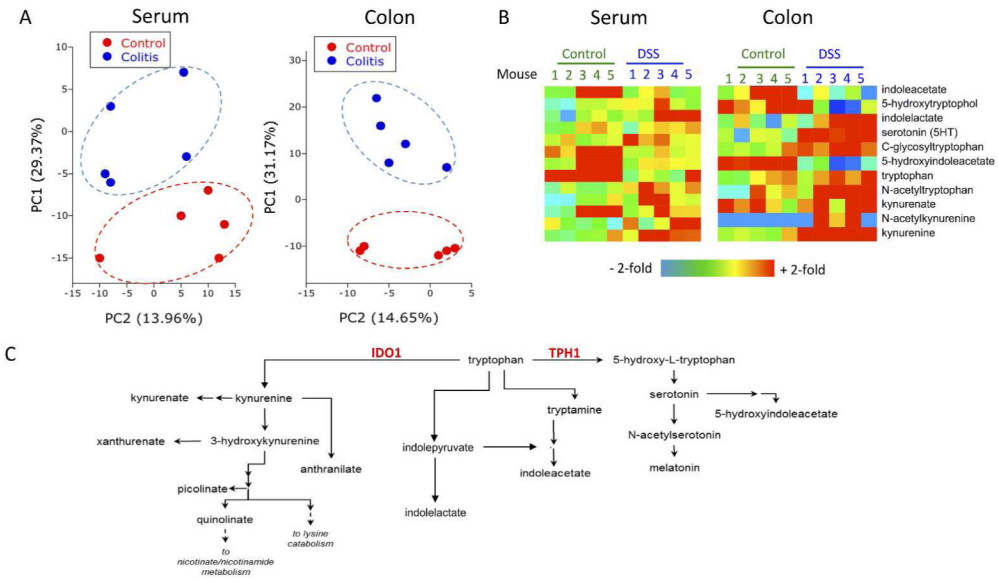

Fig. 1. Metabolomic profiling of DSS colitic mice

(A) Principal component analysis of total metabolic differences in control mice and mice receiving 3% DSS for 7 days. Metabolites were measured by Metabolon, Inc. using LC/MS and GC/MS analysis, n=5. (B) Heat map of metabolites in the Trp pathway that are altered during DSS. (C) Summary of Trp metabolism pathway including the enzymes involved in the primary metabolism of Trp to Kyn or 5-hydroxy-tryptophan.

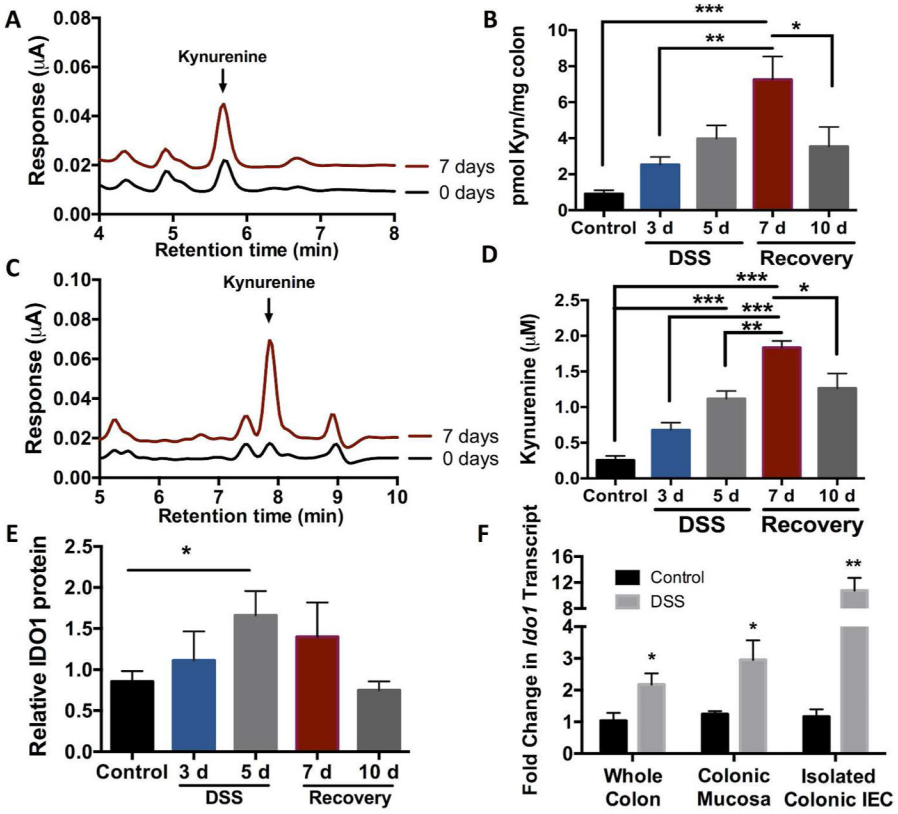

Fig. 2. Kynurenine profiling during active inflammation

(A) EC-HPLC analysis of Kyn in the colon of DSS mice at day 0 and day 7, n=5. (B) Concentration of Kyn in the colon of mice receiving 3% DSS for up to 5 days, n=5, *p<0.05, **p<0.01, ***p<0.001. (C) EC-HPLC analysis of Kyn in the serum of DSS mice at day 0 and day 7, n=5. (D) Concentration of Kyn in the serum of mice receiving 3% DSS for up to 5 days, n=5, *p<0.05, **p<0.01, ***p<0.001. (E) Western Blot quantification of IDO1 levels in the colons of mice receiving 3% DSS for up to 5 days. n=5, *p<0.05. (F) qPCR of *ido1* transcript levels in whole colon, colonic mucosal scrapings, and enriched colonic epithelial cells after 6 days of 2.5% DSS. n=5, *p<0.05, **p<0.01.

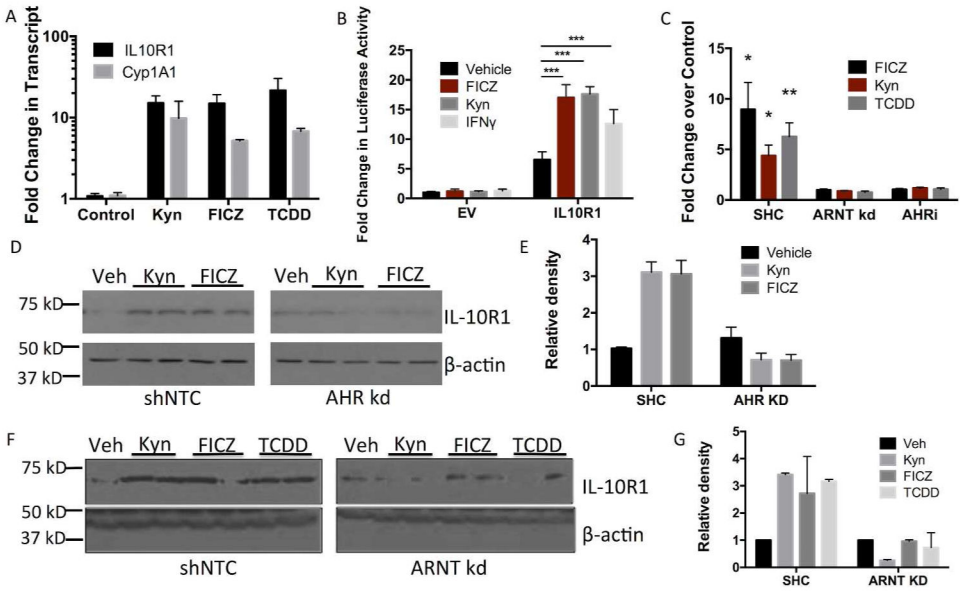

Fig. 3. IL10R1 expression in response to AHR ligands

(A) qPCR of *il10r1* and *cyp1a1* transcript levels in T84 IEC in response to AHR ligands. Confluent monolayers of T84 cells were treated with Kyn (100 μM), FICZ (250 nM), or TCDD (30 nM) for 6 h. Error bars represent the S.E.M. of five replicates. (B) Luciferase-based assay of IL10R1 promoter activity in response to AHR ligands FICZ and Kyn. IFN- γ served as a positive control. Caco-2 IECs were transfected with pGL3 containing the IL10R1 promoter region or empty pGL3 vector as control, treated for 12h with 100 μM Kyn, 250 μM FICZ, or 10 ng/mL IFN- γ and luciferase activity measured, n=3 (***p<0.001). (C) Cell surface ELISA of IL10R1 expression in shControl, shRNA ARNT knockdown, and AHR inhibitor treated Caco-2 IEC. Confluent monolayers of Caco-2 IEC were treated with 100 μM Kyn, 250 nM FICZ, or 30 nM TCDD for 24h. Error bars represent the S.E.M. of triplicate samples, *p<0.05, **p<0.01. (D) Western blot analysis of IL10R1 levels in shRNA AHR knockdown Caco-2 IEC. Confluent monolayers of Caco-2 cells containing a non-template control (shNTC) or shRNA specific for AHR were treated with FICZ or Kyn for 24 h. (E) Densitometry of the western blot analysis in Fig. 3D. Relative density of the IL10R1 bands is normalized to β-actin. (F) Western blot analysis of IL10R1 levels in shRNA ARNT knockdown T84 IEC. Confluent monolayers of T84 cells containing a non-template control (shNTC) or shRNA specific for ARNT were treated with Kyn, FICZ, or TCDD for 24 h. (G) Densitometry of the western blot analysis in Fig. 3F. Relative density of the IL10R1 bands is normalized to β-actin.

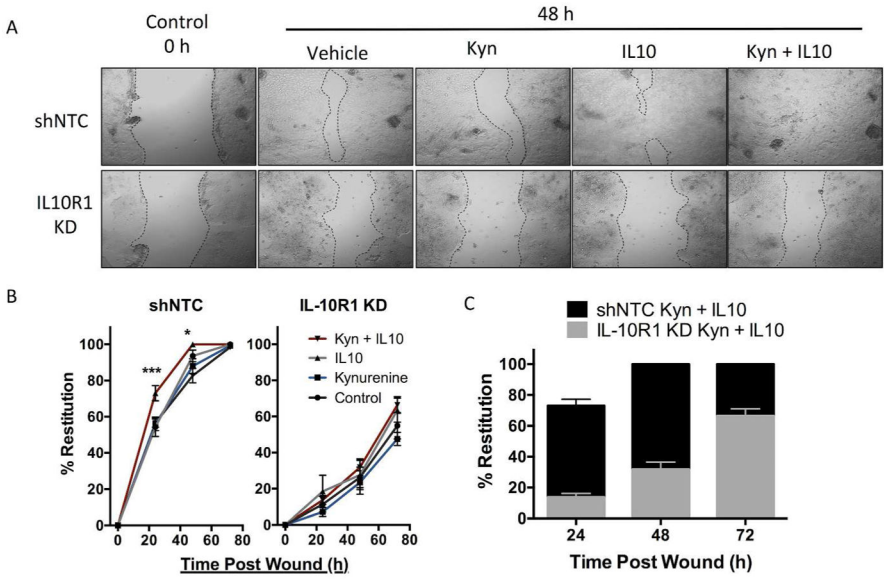

Fig. 4. In vitro scratch wound assay in T84 IL10R1 kd IEC

(A) Representative photos of T84 IEC 0 h and 48h after scratch. T84 shNTC (top) and IL10R1 kd (bottom) were treated with Kyn, IL10, or both, after wounding and monitored for 48 h. (B) Restitution of scratch wounds (y-axis) in T84 shNTC (left) and T84 IL10R1 kd (right) at 0, 24, 48, and 72h (x-axis) with control, Kyn, and IL10 treatment, n=5. (C) Comparison of shNTC (black) and IL10R1 kd (gray) wound healing with FICZ and IL10. Error bars represent the S.E.M. of triplicate measurements in five independent experiments, where *** indicates $p<0.001$ for combination of IL10 and Kyn compared to IL10 alone.

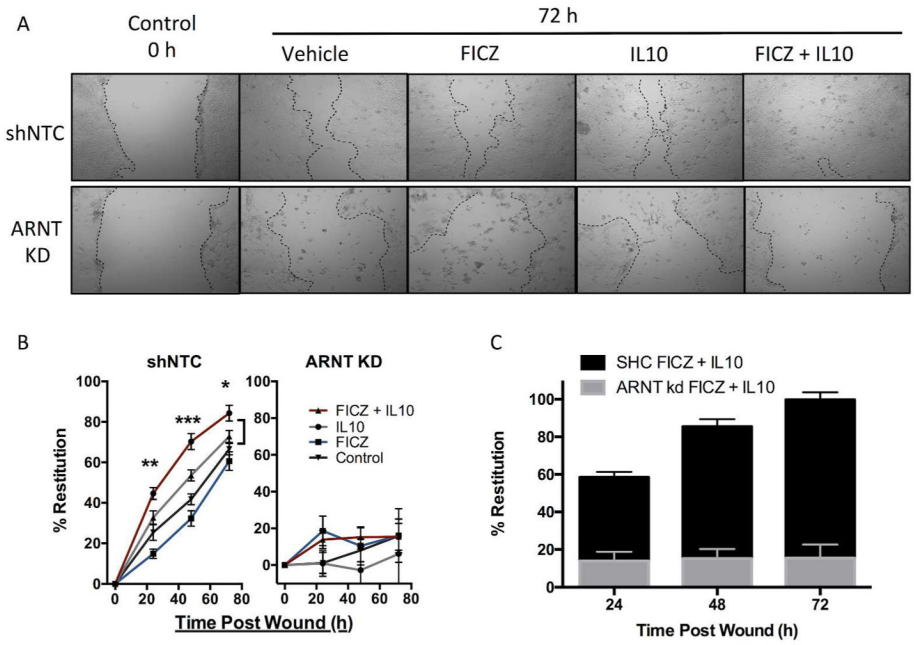

Fig. 5. In vitro scratch wound assay in T84 ARNT kd IEC

(A) Representative photos of T84 IEC 0 h and 72 h after scratch. T84 shNTC (top) and ARNT kd (bottom) were treated with FICZ (blue), IL10 (gray), or both (red), after wounding and monitored for 72 h. (B) Restitution of scratch wounds (y-axis) in T84 shNTC (left) and T84 ARNT kd (right) at 0, 24, 48, and 72h (x-axis) with control, FICZ, and IL10 treatment, n=5. (C) Comparison of shNTC (black) and ARNT kd (gray) wound healing with FICZ and IL10. Error bars represent the S.E.M. of triplicate measurements in five independent experiments, where *** indicates $p<0.0001$ for combination of IL10 and FICZ compared to IL10 alone.

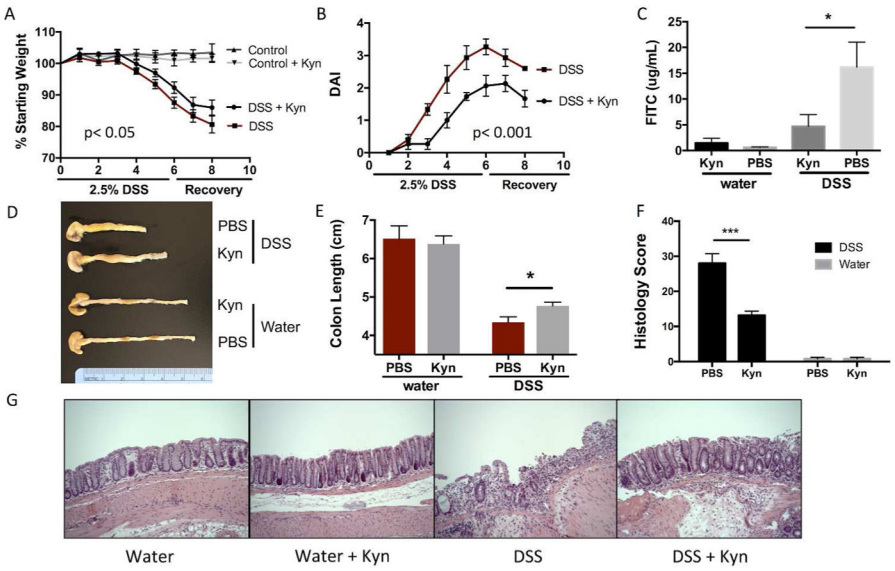

Fig. 6. Impact of Kyn supplementation on DSS colitis outcomes

(A) Weight curves during 2.5% DSS and recovery with and without Kyn administration (10 mg/kg every 48 h) n=5. (B) Disease activity scores during 2.5% DSS and recovery with and without Kyn administration (10 mg/kg every 48 h). Disease activity was measured by a combination of weight loss, stool consistency, and bleeding, n=5. (C) Intestinal permeability after 6 d of DSS and 2 d of recovery, with and without Kyn. Mice were gavaged with FITC-dextran and permeability measured by the concentration of FITC (y-axis) in the serum, n=5 *p<0.05. (D) Colon anatomy 8 d post DSS with or without Kyn. (E) Average colon length (y-axis) in mice receiving water or DSS with or without Kyn. n=5 *p<0.05. (F) Histology score after 8 d post DSS with and without Kyn, n=5 ***p<0.001. (G) Representative photos of H&E stained colon sections from DSS and control mice with or without Kyn.